

# Identification of key factors in deep O<sub>2</sub> cell perfusion for vascular tissue engineering

UMBER CHEEMA, EKTORAS HADJIPANAYI, NOOR TAMIMI, BURCAK ALP, VIVEK MUDERA, ROBERT A. BROWN

University College London, Division of Surgical and Interventional Sciences, Institute of Orthopaedics and Musculoskeletal Sciences, Tissue Repair and Engineering Centre, Stanmore Campus, London - UK

*ABSTRACT: Blood vessel engineering requires an understanding of the parameters governing the survival of resident vascular smooth muscle cells. We have developed an in vitro, collagen-based 3D model of vascular media to examine the correlation of cell density, O<sub>2</sub> requirements, and viability. Dense collagen sheets (100 μm) seeded with porcine pulmonary artery smooth muscle cells (PASMCs) at low or high (11.6 or 23.2x10<sup>6</sup> cells/mL) densities were spiraled around a mandrel to create tubular constructs and cultured for up to 6 days in vitro, under both static and dynamic perfusion conditions. Real-time in situ monitoring showed that within 24 hours core O<sub>2</sub> tension dropped from 140 mmHg to 20 mmHg and 80 mmHg for high and low cell density static cultures, respectively, with no significant cell death associated with the lowest O<sub>2</sub> tension. A significant reduction in core O<sub>2</sub> tension to 60 mmHg was achieved by increasing the O<sub>2</sub> diffusion distance of low cell density constructs by 33% (p<0.05). After 6 days of static, high cell density culture, viability significantly decreased in the core (55%), with little effect at the surface (75%), whereas dynamic perfusion in a re-circulating bioreactor (1 ml/min) significantly improved core viability (70%, p<0.05), largely eliminating the problem. This study has identified key parameters dictating vascular smooth muscle cell behavior in 3D engineered tissue culture. (Int J Artif Organs 2009; 32: 318-28)*

*KEY WORDS: Vascular smooth muscle cells, Oxygen, Collagen*

## INTRODUCTION

New alternatives for the replacement of human blood vessels are becoming increasingly necessary to address growing clinical problems associated with aging, trauma and vascular disease (1). Grafts based on synthetic materials and xenogenic or autologous tissues are hampered by limitations of rejection, thrombosis, chronic inflammation, fibrosis and limited supply (2). Tissue engineered grafts have the potential to solve at least some of these problems. Successful approaches have included the use of multi-cell layers to form myocardial patches and tubes (3), cell-seeded blood vessel implants (4, 5) and decellularized tissues composed of native matrix proteins (6, 7). Once assembled, a plethora of conditions including mechanical loading and media flow perfusion etc. can be controlled with the aim of optimizing eventual functional properties (1, 8). However, selection, monitoring and application of

such 3D culture control parameters have not always been soundly or systematically based. Interestingly, this bottom-up process engineering of tissue function has also informed our understanding of physiology, growth and repair processes.

Native 3D structure of most tissues is characterized by specific and essential 3D cell-matrix architecture at the micro- and nano-scales (9, 10). By culturing cells in appropriate spatial locations and by engineering the density and fibrillar architecture of their supporting Extracellular matrix (ECM), this 3D tissue geometry can be mimicked (11-15). Attempts to build such spatially biomimetic systems have been developed around 3D collagen gels (16) in which the rapid fabrication process of plastic compression (PC) is used to produce controlled collagen densities to levels comparable to native tissue (12). However in the process of solving many of the basic questions of directly engineering simple, living collagenous tissues with biomimetic structu-

re, it is now important to tackle the perceived, but poorly understood question of deep cell perfusion/viability.

Given the obvious limitations of mass transport (without microvascular perfusion) in 3D culture, a clear evidence-based understanding of the formation and effects of prevailing  $O_2$  tension gradients on deep cell behavior is essential (17-21). Previous work has examined the formation of such diffusional oxygen gradients in statically cultured cardiac constructs and their effects on spatial cell distribution and cell viability (18). Similarly, vascular smooth muscle cells (SMCs) are, by their nature, likely to generate steep  $O_2$  gradients and it is key to know their responses in different parts of the vessel wall, both across (radial) and along (longitudinal) the vessel axis (22).  $O_2$  tension *in vivo* is high in arterial blood but reduces rapidly with distance away from the lumen (radially) into the surrounding adventitia. Cells in specific spatial positions through the vessel wall are habitually exposed to a range of  $O_2$  tensions governed by their own metabolic activity and density. We have previously found that in matrix-rich ECM systems diffusion distance and matrix density contribute to, but do not dominate, gradient formation (13). Critically, the  $O_2$  requirement varies for different cell types, cell behaviors and tissues. Indeed, while respiratory epithelium and outer skin layers are exposed to atmospheric levels of  $O_2$  (21%; 160 mmHg), physiological hypoxia (1-10%  $O_2$ ; 7.6-76 mmHg) is by far the most common natural environment for most mammalian tissues (23).

Local  $O_2$  tension can itself regulate some cell-based events, such as angiogenic signaling (24, 25). Hypoxia Inducible factor-1 alpha (HIF-1 $\alpha$ ) is a potent transcription factor (24) for a variety of angiogenic markers, primarily vascular endothelial growth factor (VEGF), and a major stimulus of this is low  $O_2$  tension or physiological (7.6-76 mmHg  $O_2$ ) and pathological (<7.6 mmHg  $O_2$ ) hypoxia (26). In most tissues, HIF-1 $\alpha$  induces and regulates angiogenesis by controlling growth factor expression involved in the growth of new capillaries. However, in avascular cartilage, HIF-1 $\alpha$  upregulates the synthesis of major matrix components, such as collagen type II, suggesting that  $O_2$  tension regulates cell signaling in a cell/tissue specific manner.

A substantial body of literature already suggests that the wall of pulmonary blood vessels is home to a number of distinct cell phenotypes, including inner and outer layer pulmonary arterial smooth muscle cell (PASMC) types (27-29). Outer PASMCs (i.e., furthest from the lumen) are not only more contractile, they respond to chronic hypoxia by reducing contractility. In contrast, inner PASMCs (adjacent to the vessel lumen) show no change in their contraction profile (27). It is possible, therefore, that cells in specific

spatial locations within tissues, in this case the vascular media, develop and adapt to utilize defined ranges of  $O_2$  tension. Unintended or uncontrolled tendencies for  $O_2$  gradients to produce locally inappropriate smooth muscle cell phenotypes would then be a serious problem in engineering vascular structures. Consequently, it is important to use biomimetic engineering to understand and generate similar spatial  $O_2$  gradients in artificial 3D tissues where they are functionally important.

Blood vessel engineering is a particularly stark example of potential 3D construct mismatch *in vivo*. In this, as in culture,  $O_2$  nutrient gradients form from the surface to the core of the 3D construct. In contrast, even the earliest naturally perfused vessel will have a reverse gradient from the core to the outer layer. This mismatch in  $O_2$  nutrient gradient direction has to be carefully considered when designing and engineering 3D *in vitro* vascular models. Indeed, given the possibility that different cell types (in this case vascular smooth muscle cells in the media and fibroblasts in the adventitia) respond differently to varying  $O_2$  tension, cell spatial positioning would be critical. In this study we have quantified  $O_2$  consumption by PASMCs seeded under a range of conditions in dense 3D collagen tubular constructs to establish a working experimental model of the system. We hypothesize that  $O_2$  consumption by resident cells, rather than matrix density /diffusion coefficient or diffusion path length will effectively generate natural (i.e. biomimetic) transverse  $O_2$  gradients from the outer wall surface of the construct to the core (lumen). In this study we have dissociated between these three elements and have correlated  $O_2$  consumption gradients with cell density to test if exposure of core cells to lower  $O_2$  tension reduces cell survival, measured as cell viability along the radial consumption gradient, under both static and dynamic perfusion culture conditions. Furthermore, to show how different cell types behave in terms of  $O_2$  consumption, we quantitatively compared PASMC responses to those of human dermal fibroblasts (HDFs), cultured under identical conditions in the same 3D model (13) up to 6 days in culture.

## MATERIALS AND METHODS

### *Cell preparation and expansion*

Pulmonary arterial smooth muscle cells (PASMCs) were isolated from elastic intrapulmonary arteries from five normal 14 day-old Large White piglets. All piglets were kept in accordance with the NIH (USA) *Guide to the Care and Use of Laboratory Animals* (1996) and Home Office (UK) regu-

lations. Immediately after death, the lungs were removed and 1 cm lengths of the main intrapulmonary artery dissected from both lower lobes. PASMCs were isolated by dissection and enzyme dissociation from the outer (50%) medial layers, as described previously (30). The cells were grown in F12-Hams medium supplemented with 20% fetal calf serum (First Link, West Midlands, UK), 2 mM glutamine and penicillin/streptomycin (1000 U/mL; 100 mg/mL, Gibco Chemicals) and used between passages 3 and 8. For removal of cells from monolayer culture, flasks containing cells were washed with PBS, and incubated with trypsin (0.5% in 5 mM EDTA, Invitrogen, UK) for 5 minutes at 37°C.

### Preparation of 3D plastic compressed (PC) collagen gel constructs

Once detached, cells were counted and embedded in 3D collagen type I gels. Collagen gels were set in a mold with dimensions 2.2 (width) x 3.3 (length) x 1 cm (height). For collagen gel preparation, 0.5 mL of 10xEagles MEM solution (Gibco Life Technologies, Paisley, UK) was added to 4 mL rat-tail type I collagen (First Link, UK Ltd) in 0.1 M acetic acid, protein concentration 2 mg/mL, neutralized with 1 and 5 M NaOH, using the indicator color changes from yellow to cirrus pink. This gel preparation was added to a 0.5 mL cell suspension and set in the mold at 37°C for 30 minutes. Gels were then removed from the mold and routinely compacted by a combination of compression and blotting between layers of supporting nylon mesh and filter paper sheets (12). Collagen gels were loaded with a 120 g mass for 5 minutes at room temperature, to provide flat collagen sheets (96.4±8.7µm thick (12)) protected between two nylon meshes. Importantly, plastic compression has previously been shown not to significantly reduce cell viability (12). These dense, dehydrated collagen sheets were then rolled around a 1 mm external diameter hollow mandrel (0.8 mm internal diameter) to produce tight spirally wound tubular constructs, ~4 mm in external diameter, 21 mm in length (Fig. 1a). Use of a tubular construct model in this case enabled rapid and precise layering of collagen sheets which would be technically difficult with a planar model. Construct radial (wall) thickness was varied between ~1.5 mm and ~2 mm by controlling the starting sheet length of the collagen sheet, hence the number of spiral layers; PC collagen sheets of 3 cm in length produced 15 layer spiral constructs, corresponding to 1.446±0.13 mm radial wall thickness (each layer was 96.4±8.7µm thick), while sheets of 4.5 cm long produced 20 spiral layers and 1.93±0.17 mm radial wall thickness. There was no significant change

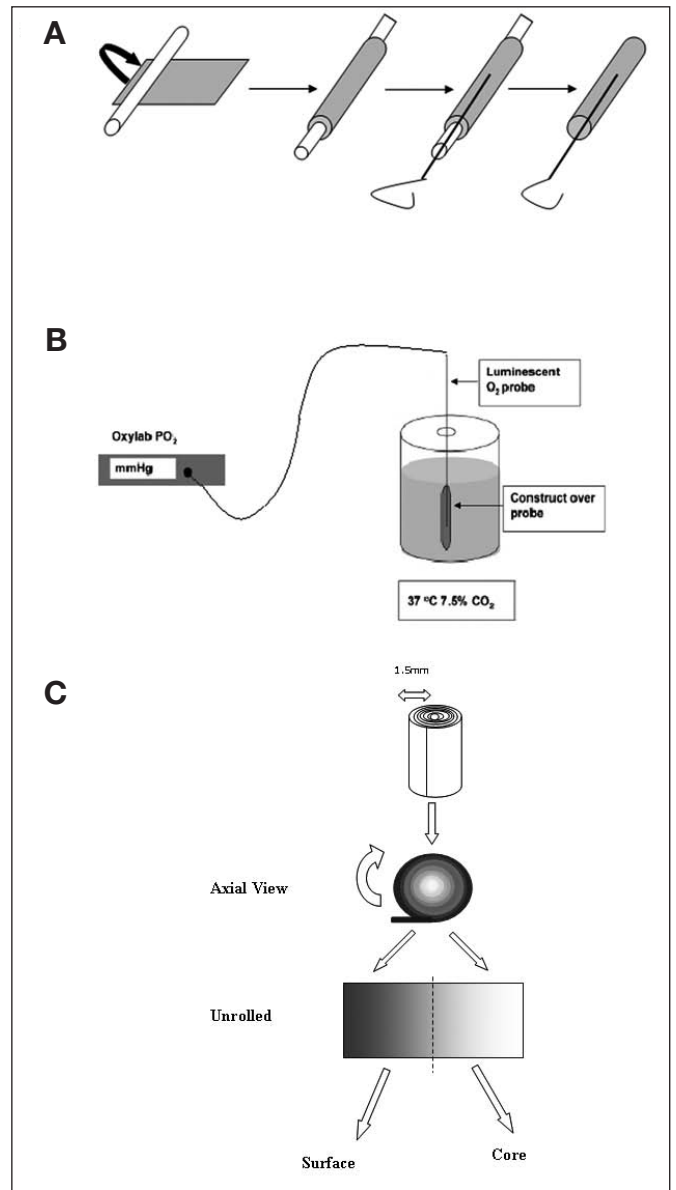


**Fig. 1** (a) Schematic of development of tubular spiral collagen constructs. Compressed collagen sheets were spiraled around a mandrel and an O<sub>2</sub> probe was inserted into the mandrel before the mandrel was withdrawn, leaving the probe in the center of the construct. Constructs were then sealed at both ends using cyanoacrylate glue, which also ensured that spiral constructs were kept from unwinding in culture. (b) Schematic of the experimental set up, with O<sub>2</sub> probe in the centre of a spiraled plastic compression construct. Constructs were cultured in 50 mL media. (c) Assessment of cell viability involved unrolling 3D constructs and dissecting 2 regions corresponding to the core and surface of the spiral constructs.

in radial wall thickness of cell-seeded constructs over a 3-day culture period (data not shown). Required cell densities were calculated in direct proportion to the initial cell seeding density and fluid loss during plastic compression.

Final cell density was calculated as: initial cell density x fold volume change during PC. Hence for a typical initial gel volume of 5 mL, and collagen concentration of 0.2%, this increased to 11% following compression (measured by dry/wet weight ratio), corresponding to a 58-fold increase. Since all seeded cells remain within the PC collagen gel, final cell density increased in proportion from 200,000 cells/mL (or 1 million cells/construct) to 11.6 million cells/mL, and from 400,000 cells/mL (or 2 million cells/construct) to 23.2 million cells/mL (13).

### Oxygen monitoring

Fiber-optic O<sub>2</sub> probes (Oxford Optronix, Oxford, UK) were inserted into the lumen of acellular and cell-seeded 3D tubular constructs by first inserting the probe into the mandrel, positioning it halfway along the long axis of the construct and withdrawing the mandrel to leave the sensor probe (280 µm diameter) in the construct lumen (1 mm diameter) (Fig. 1a). The constructs were then sealed at both ends using cyanoacrylate glue. In addition to preventing O<sub>2</sub> diffusing longitudinally into the construct from the two ends, sealing the ends also ensured that spiral constructs were kept from unwinding in culture and that the O<sub>2</sub> probe was secured in place to prevent its longitudinal and radial movement during the experiment. Hence, a diffusion length of >1 mm was dominant throughout the construct, radially across the tube wall from lumen to surface. The 3D monitoring set-up is shown schematically in Figure 1b. Three-dimensional samples were cultured statically in standard 100 mL universal tubes. Constructs attached to O<sub>2</sub> probes were bathed in 50 mL complete medium composed of F12 Ham's media supplemented with 10% (v/v) fetal calf serum (FCS, First Link, Birmingham, UK), 2 mmol/L glutamine (Gibco Life Technologies, Paisley, UK), 1,000 U/mL penicillin and 100 mg/ml streptomycin (both from Gibco Life Technologies, Paisley, UK). There was no change of medium during each experiment. The tip of the sensor probe incorporates an O<sub>2</sub>-sensitive luminescent compound within an O<sub>2</sub>-permeable matrix. Quenching of the luminescence by molecular O<sub>2</sub> allows the luminescence emission lifetime to be used as a read-out of O<sub>2</sub> tension in immediate surroundings. The calibration of the optical O<sub>2</sub> probe is accurate to 0.7 mmHg, with exceptional stability over 6 days at the slowest sampling rate (13). Readings were taken continuously in real-time. O<sub>2</sub> tension in the construct core refers to measurements recorded within the construct lumen, while O<sub>2</sub> tension at the construct surface refers to O<sub>2</sub> tension recorded in the surrounding media. After each experiment, the probe reading was taken in the external medium to confirm

minimal drift in response. Fiber-optic probes were used in conjunction with an OxyLab pO<sub>2</sub>ETM system (Oxford Optronix Ltd, Didcot, UK) coupled to an A/D converter (12 bit) with data collection to Labview (National Instruments, TX, USA). Results are presented as partial pressure values (i.e., pO<sub>2</sub>) in mmHg (e.g., 7.6mmHg corresponds to 1% O<sub>2</sub>). To calculate O<sub>2</sub> consumption rate (mmHg O<sub>2</sub>/h) in cell-seeded constructs, the hourly O<sub>2</sub> tension in cell-seeded constructs was subtracted from the 24-hour average O<sub>2</sub> tension in acellular constructs.

### Cell viability

Cell viability was qualitatively assessed using the Live/Dead Viability/Cytotoxicity Kit (L-3224; Molecular Probes, Eugene, OR, USA) based on the simultaneous staining of live and dead cells with calcein AM and ethidium homodimer (EthD-1), respectively. Quantitative analyses were carried out with Live/Dead Reduced Biohazard Viability/Cytotoxicity Kit (L-7013; Molecular Probes, Eugene, OR, USA) according to the manufacturer's protocol. SYTO-10, a green fluorescent nucleic acid stain and Dead Red (ethidium homodimer-2) were used, and, after capturing images, live/dead nuclei were counted to give % cell viability. Spiral constructs were first unrolled and then cut into 2 sections, corresponding to core and surface regions and stained (Fig.1c). Viability of cells in each construct was performed independently from the O<sub>2</sub> measurements. Representative areas were chosen in two regions (core and surface) of PC constructs and were visualized using confocal microscopy (Bio-Rad Radiance 2100; Carl Zeiss Ltd, Hertfordshire, UK). Five or more random fields were viewed per section with at least 3 samples for each experimental condition.

### Dynamic perfusion cell culture

Collagen spiral constructs were produced by rolling PC cell-seeded collagen sheets round a solid mandrel (1 mm diameter) and sealing the ends of each construct using cyanoacrylate glue. The mandrel supporting the constructs was then inserted into a silicone tube (8 mm internal diameter, 80 cm length) connected at one end to a peristaltic pump (Masterflex, Cole Parmer) and at the other end to a 500 mL media reservoir. The flow rate was adjusted so that the constructs were perfused with medium around the outer construct surface (i.e., no medium flow through the lumen) at a constant rate of 1 ml/min throughout the culture periods of 24 hours or 6 days. During the culture period, 500 mL of complete medium was re-circulated.

### Statistical analysis

The t-test was used for all analyses, as a maximum of 2 groups was used per analysis; a minimum of 3 samples was tested for all conditions. Error bars indicate standard deviation from the mean.

## RESULTS

We first measured O<sub>2</sub> diffusion into the core of cell-free PC collagen tubular constructs (~1.5 mm radial wall thickness). This kind of validation and calibration studies without cells (Fig. 2a) provided a steady-state base level O<sub>2</sub> tension at the core and surface (~148 mmHg) over 24 hours (note that the fluctuations in core O<sub>2</sub> tension over 24 h were not statistically significant,  $p > 0.05$ ). This core level was not significantly different from the external medium (data not shown), indicating a “zero” gradient with free O<sub>2</sub> diffusion through the nano-fibrillar collagen matrix of the wall. This concurs with our previous work showing a high O<sub>2</sub> diffusion coefficient through this dense collagen (unpublished data). In contrast, cellular constructs (~1.5 mm radial thickness) exhibited time-dependent O<sub>2</sub> depletion in their core over a period of 24 hours (Fig. 2a). O<sub>2</sub> tension fell rapidly over 0 to 5 hours depending on cell density, reaching  $10 \pm 6.2$  mmHg for high cell density constructs ( $23.2 \times 10^6$  cells/mL) and  $80 \pm 11.7$  mmHg at the low density ( $11.6 \times 10^6$  cells/mL). The 2- and 8-fold decrease in O<sub>2</sub> tension at low and high cell densities, respectively, was significant ( $p < 0.05$ ) indicating that cell O<sub>2</sub> consumption (i.e., the number of cells consuming O<sub>2</sub> along the diffusion path) was a central determinant of core O<sub>2</sub> tension in the system at 24 hours. Core O<sub>2</sub> tension was inversely proportional to cell density. Figure 2b illustrates the relationship between cell density and O<sub>2</sub> consumption rate, with constructs seeded at twice the cell density having an O<sub>2</sub> consumption rate that was 2-fold greater over the 12- to 24-hour period of culture. The initial consumption rate (0-5 h) was 3-fold higher at the high cell density, perhaps due to pre-adaptational differences in core cell metabolism at different O<sub>2</sub> tensions (going from culture hypoxia to tissue-like normoxia). Importantly, core O<sub>2</sub> tension was found to be stable over extended periods, from 24 to 72 hours, at ~20 mmHg (Fig. 2c). This contrasts with the same system previously established using HDFs, which adapted over the 24- to 72-hour period to reduce O<sub>2</sub> consumption, such that core O<sub>2</sub> tension rose to 65 mmHg by 30 hours (13). This 3-fold difference between the PASMCM and HDF O<sub>2</sub> level became statistically significant at 40 hours (Fig. 2c).

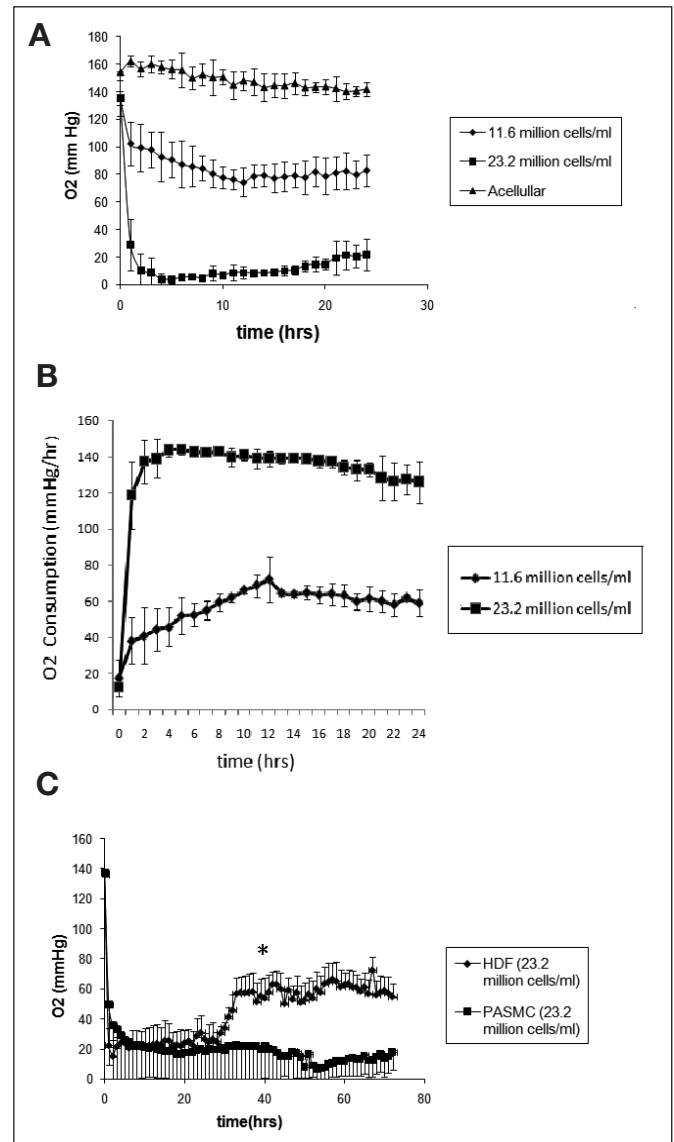


**Fig. 2 - (a)** O<sub>2</sub> tension in the centre of acellular and PASMCM-seeded spiral constructs cultured for 24 h. Two different cell densities were measured, 11.6 million cells/mL and 23.2 million cells/mL (average of  $n=5$  for each data set is presented here). Time-zero is taken as the time point when the probe was positioned in the construct. **(b)** Rate of O<sub>2</sub> consumption within constructs seeded with 11.6 million cells/mL and 23.2 million cells/mL and cultured for 24 h. **(c)** O<sub>2</sub> tension in the centre of spiral constructs seeded with 23.2 million cells/mL and cultured for 3 days ( $n=3$ ). Comparative HDF data has been derived from Cheema et al (13), \* $p < 0.05$ .

We also tested the effect of increasing diffusion distance on core O<sub>2</sub> tension within the lower cell density constructs ( $11.6 \times 10^6$  cells/mL). This compared the effects of increasing the diffusion distance (i.e., construct wall radial thickness) from ~1.5 mm to ~2 mm. This not only resulted in increased wall thickness, but also increased the total num-

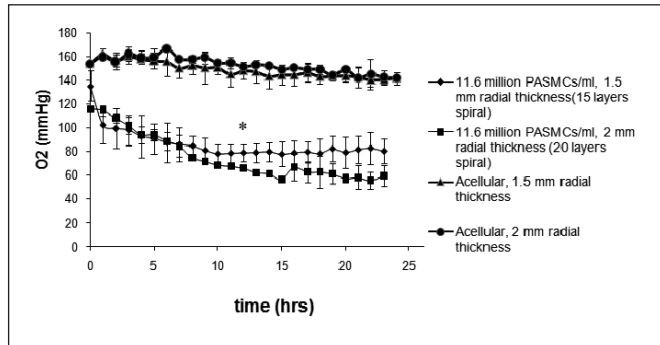


**Fig. 3** -  $O_2$  tension in the centre of acellular spiral constructs and constructs seeded with 11.6 million cells/mL and cultured for 24 h. Constructs had a radial thickness of 1.5mm (15 layers spiral) or 2 mm (20 layers spiral), \*  $p < 0.05$ .

ber of cells along that diffusion path (i.e., the consumption gradient increased with distance). Figure 3 shows that for acellular constructs, increasing the diffusion distance had no significant effect on core  $O_2$  tension. For cell-seeded constructs, an increase in diffusion and consumption path-length of 33% resulted in an increase in  $O_2$  consumption (by ~30%) and reduction in core  $O_2$  tension (marked here as significant after 12 h,  $p < 0.05$ ). Importantly, even though the increase in diffusion/consumption path generated a proportionately lower core  $O_2$  tension post 12 hours, rather than an altered initial rate of consumption (0-10 h slope).

We previously established that human dermal fibroblasts (HDFs) seeded at  $23.2 \times 10^6$  cells/mL within compressed collagen constructs retained high (80%) core cell viability for up to 5 days in culture (13). This was compared with the effect of physiological hypoxia on PASCs by measuring the difference in cell viability between core and surface cells (high density cultures) over 0-6 days. Exposure of PASCs to the lowest levels of  $O_2$  (~10 mmHg) in the core had no significant effect on 24-hour cell viability (Fig. 4a), which was over 95% in both the core and surface of the construct, indicating that this cell type is not rapidly susceptible to short term hypoxia. However, after 6 days of static culture, there was a significant reduction in cell viability both at the construct core (55%) and surface (75%) ( $p < 0.05$ ) (Fig. 4a). This decrease in cell viability was accompanied by a gradual increase in core  $O_2$  tension from 20 mmHg at 72 hours to 100 mmHg at day 6, as overall  $O_2$  consumption was reduced, apparently due to the reduced cell number (Fig. 4b). It is important to note, however, that this increase in core cell death, at low  $O_2$  tension, was accompanied by a smaller but still significant level of cell death at the surface where  $O_2$  was not depleted.

We hypothesized that introduction of forced flow of medium to this static system would reduce  $O_2$  gradient formation. Constructs were then tested under dynamic perfusion for cell survival. Dynamic perfusion culture of high cell density constructs for 6 days significantly improved core cell viability at day 6 (from 55% in static culture to 70% in dynamic perfusion culture,  $p < 0.05$ ) (Fig. 5). Six-day surface cell

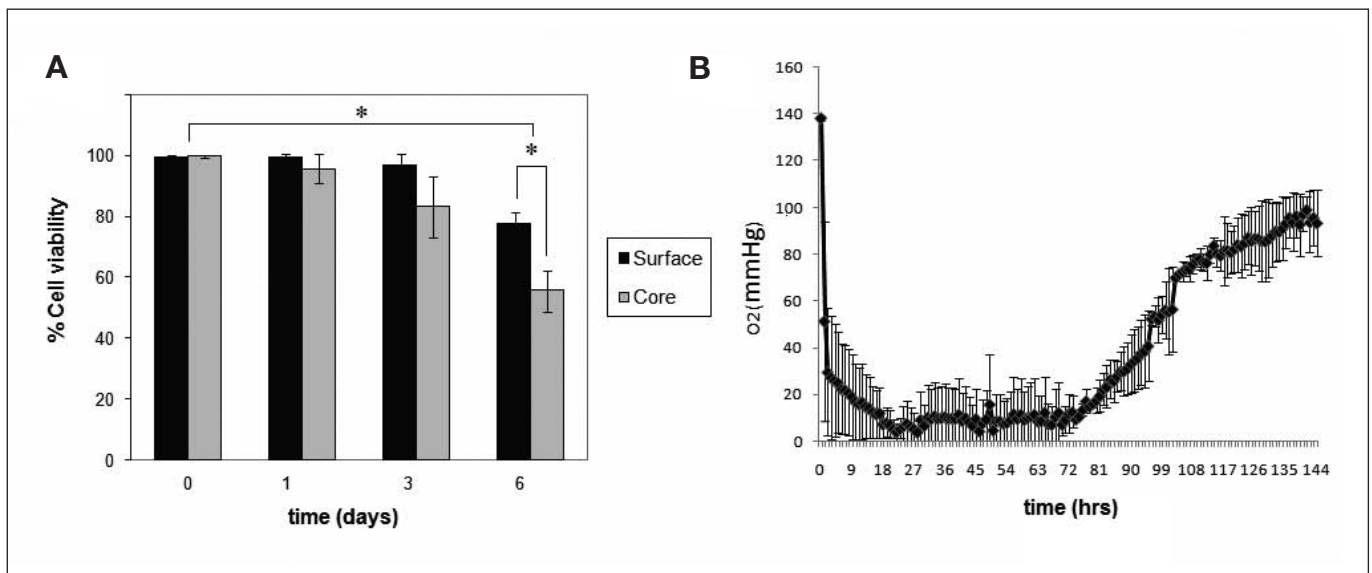


**Fig. 4** - (a) Cell viability measured at time zero and then at 1, 3 and 6 days in static cultures (23.2 million cells/mL), \*  $p < 0.05$ . (b)  $O_2$  tension in the centre of spiral constructs seeded with 23.2 million PASCs/mL and cultured for 6 days.

viability (88%) was also increased relative to static (75%) but this was not statistically significant, being effectively the same as short-term (day 1) with minimal cell death (Fig. 5). Dynamic perfusion culture, however, did not abolish the difference in cell viability between core and surface, observed with static culture, which remained statistically significant after 6 days ( $p < 0.05$ ). The observed increase in long-term core cell viability under perfusion culture was in agreement with the finding that cellular O<sub>2</sub> consumption imposed a limitation in core O<sub>2</sub> availability and compromised cell survival.

## DISCUSSION

The field of vascular tissue engineering is growing, with many groups focusing on understanding and re-creating *in vitro* environments for the successful culture of appropriate cell types. A blood vessel comprises three spatially distinct layers; adventitia (fibroblast component), media (smooth muscle cell component), and an inner endothelial luminal layer (31). Groups have developed vascular models and grafts by using different combinations of cell layers. Niklasson and colleagues have focused on using polyglycolic acid (PGA) scaffolds for seeding a smooth muscle cell layer with an inner endothelial layer (8). In comparison L'Heureux and colleagues have focused on using cell sheets of fibroblasts round a decellularized internal membrane and an inner endothelium (2, 4). In the present study we have focused on understanding how to optimally grow vascular smooth muscle cells in dense 3D collagen scaffolds and have compared the required O<sub>2</sub> conditions with those of fibroblast studies from previous work using the same system (13). Cell-specific optimization of O<sub>2</sub> conditions could provide an important tool to successfully engineer each segment component of a vessel wall.

The major limiting factor resulting in O<sub>2</sub> depletion in the core of 3D collagen constructs was cell consumption of O<sub>2</sub> and not a limitation of O<sub>2</sub> diffusion caused by extended diffusion path-length through ECM (up to 1.5-2 mm, as tested in this model). Previous research carried out on thick fibrin matrices has indicated that gel thickness, in the order of centimeters, was not a limiting factor for O<sub>2</sub> diffusion (32). Such components of native ECM (i.e., collagen, fibrin) have already been used in direct applications as biomimetic tissue engineering scaffolds. Differentiating between diffusional and cell consumption limitations, in terms of nutrient supply to the scaffold core, is critical for the design of bioreactors where constructs are cultured prior to implantation.

It is important to note that while the current model's tubu-

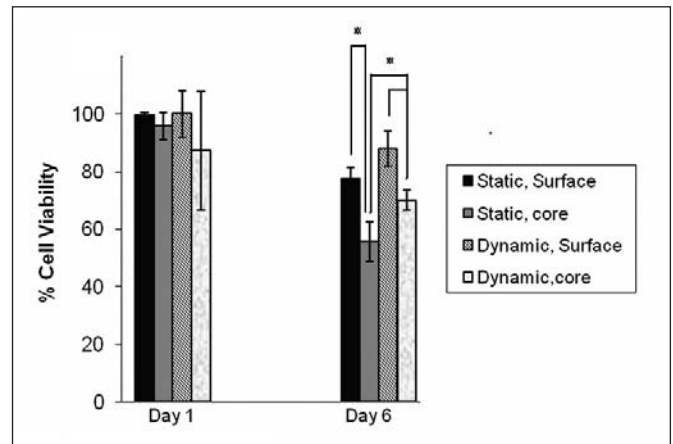


**Fig. 5** - Cell viability, as measured by live/dead assay for constructs seeded with 23.2 million PSMCs/mL and cultured for 1 and 6 days under static and dynamic perfusion culture conditions, \*  $p < 0.05$ .

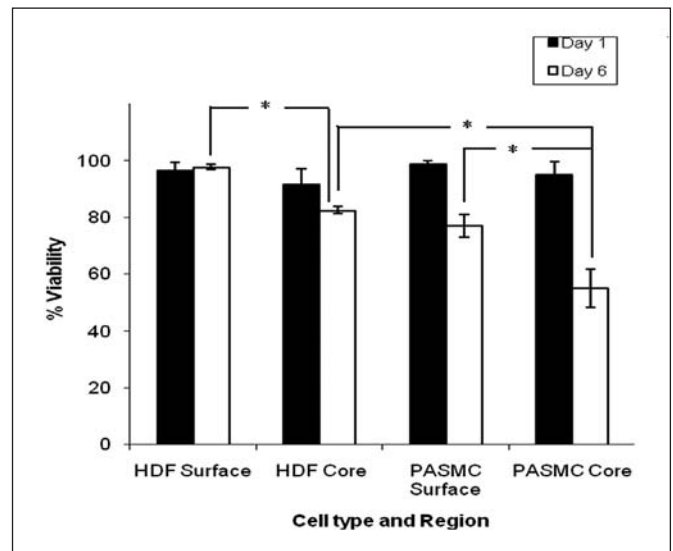


**Fig. 6** - Cell viability, as measured by live/dead assay for constructs seeded with HDFs and PSMCs at 23.2 million cells/mL and cultured for 1 and 6 days under static culture conditions, \*  $p < 0.05$ . Comparative HDF data has been derived from Cheema et al (13).

lar geometry mimics "3D vascular tissue geometry", it effectively creates radial O<sub>2</sub> gradients which are opposite to the natural gradients. The use of a tubular model in this case did not aim to reproduce the directional anisotropy of *in vivo* gradients, but made it feasible to engineer a 3D model tissue where cell density and radial thickness could be easily and predictably controlled (12), in order to examine their effects on spatio-temporal changes in O<sub>2</sub> tension.

There was a direct linear relation between cell density and O<sub>2</sub> consumption by 24 hours, however, the initial (0-5

h) rate of  $O_2$  consumption was not directly proportional to cell density. In fact, for the higher cell density (double that of the lower cell density) initial  $O_2$  consumption was 3-fold higher. This finding seems to be in agreement with the well-established principle that rates of energy metabolism are dependent not only on a single substrate but on the entire nutrient-metabolite milieu. For instance, oxygen uptake is enhanced at low glucose concentrations (the Crabtree effect (33)). Oxygen consumption rate also varies with oxygen concentration and pH (34). The linear relationship which develops within 24 hours may represent an adaptive response by cells to the surrounding  $O_2$  environment. There is likely to be an iterative feedback response with regards to  $O_2$  consumed and  $O_2$  available, which in turn will regulate the cellular metabolic response and other changes in gene expression, primarily extracellular matrix production and up-regulation of angiogenic signals (35, 36). It is important to note that smooth muscle cell densities in the present study are comparable to those used in previous vascular engineering studies ( $40\text{--}100 \times 10^6$  cells/mL) (8).

$O_2$  consumption by HDFs, cultured in the same 3D system, showed that for a seeding density of  $23.2 \times 10^6$  cells/mL,  $O_2$  tension was not significantly different compared to that observed with PSMCs after 24 hours (13). While core  $O_2$  tension ( $\sim 20$  mmHg) was found to be stable over extended periods, between 24 and 72 hours for PSMCs, this was not the case with HDF cultures where core  $O_2$  tension rose back to 65 mmHg by 30 hours (Fig. 2c). As mentioned above, this is likely to be due to differences in cell metabolism and  $O_2$  utilization between the two cell types, with HDFs appearing to adapt to hypoxia by reducing their  $O_2$  consumption. These findings suggest that PSMCs are high consumers of  $O_2$  and that cell phenotype, as well as cell density, is an important determinant of  $O_2$  consumption.

Constructs of varying radial thickness (15 vs. 20 layers, corresponding to  $\sim 1.5$  vs.  $\sim 2$  mm thickness) and thus of varying diffusion and consumption path length, exhibited different plateau values of  $O_2$  tension. This response, however, was characterized by a 12-hour lag phase. Given the high diffusion coefficient of  $O_2$  through acellular collagen (unpublished data), the 33% increase in terms of material thickness should minimally affect the rate of diffusion, which was in agreement with experimental data. This indicates that the 12-hour lag phase observed here was a function of the cell  $O_2$  consumption gradient established in this system. Controlling construct thickness (i.e., number of cell-seeded layers), as well as cell density (i.e., number of cells per layer) could thus provide an additional means for controlling the rate of  $O_2$  consumption through a construct. This ability to selectively and predictably "tune"  $O_2$  distribution and local

tissue perfusion within a 3D construct could have important implications for the layer-by-layer (e.g., cell-sheet and matrix-sheet engineering) approach which has been pursued by a number of groups due to its architectural relevance to blood vessel structure (4, 25, 37).

While our data suggests that in cell-seeded collagen constructs the formation of  $O_2$  gradients was the result of cell consumption, it is possible that changes in material properties through cell-mediated matrix remodeling could also have contributed at later stages to changes in  $O_2$  diffusion (38). Indeed, cell-seeded constructs cultured for 2 days had a 2.5 fold higher stiffness modulus ( $p < 0.05$ ) compared to day 0 cell-seeded constructs (data not shown). Within such a short time period, however, and given the high initial stiffness (1.8 MPa (12)) of acellular compressed collagen matrix ( $\sim 50$  fold higher than the stiffness of uncompressed collagen hydrogels-40 KPa (39), which undergo cellular remodeling within 24 h), this increase in stiffness was likely contributed by cytoskeletal elements (cytoskeletal stiffness) which act additively to matrix stiffness (40). However, it is possible that over longer periods of culture, cell-mediated matrix remodeling (increase in density of collagen filaments or cross-linking between collagen fibrils, namely, change in the porosity of the material) could have a significant effect on  $O_2$  diffusion (41).

Viability of PSMC in the core of high cell density constructs exposed to levels  $< 10$  mmHg of  $O_2$ , remained high ( $\sim 80\%$ ) up to 3 days, however by day 6 this level decreased to 58%. We have established, then, that PSMCs can survive physiological hypoxic conditions for at least 24 hours. While PSMC exposure to hypoxia did not result in rapid cell death (i.e., within 24 h), continued exposure did kill cells, probably until the core  $O_2$  rose again, sparing the remaining cells. It is important to note that while plastic compression has previously been shown not to significantly reduce cell viability (12), at such high seeding cell densities no cell proliferation occurred (39). This implies there was a net reduction in cell number within constructs at 6 days. Not surprisingly, this was accompanied by a gradual increase in core  $O_2$  tension, in agreement with reduced overall  $O_2$  consumption, representing a natural feedback mechanism, likely to mirror that found *in vivo*. A previous study has shown that the environment within polymer scaffolds containing transplanted hepatocytes was hypoxic ( $p O_2 < 10$  mmHg) after 5 days *in vivo* (42), indicating that the detrimental effect of hypoxia on long-term cell survival is not limited to *in vitro* culture. However, this study highlights that the reported effect of hypoxia on cell viability has to be treated with caution, as different cell types show different consumption and sensitivity to reduced  $O_2$  tension. As discussed above, HDFs can adapt to



hypoxia by reducing their O<sub>2</sub> consumption, resulting in significant long-term viability (Fig. 6). This has important implications for engineering complex tissues where two or more cell types are present (such as blood vessels).

In our 3D model, in addition to O<sub>2</sub> availability, the diffusion of key higher molecular weight nutrients (i.e., glucose) may be a limiting factor for cell survival. Glucose diffusion coefficients have previously been established and this is not found to be limiting for cells in the same 3D model (43). While glucose diffusion might not be a limiting factor, static culture of cells within this 3D model does produce a glucose consumption gradient from the construct surface to its core within 24 hours (unpublished data), implying that low core glucose levels could have contributed to decreased core cell viability. However, previous work has shown that fibroblasts exposed to hypoxia become tolerant to glucose starvation as they switch to amino acids as an energy source (44). Whether PSMCs respond in a similar manner remains to be examined.

It is also important to consider the possibility that cells cultured statically (without circulation of culture medium) were exposed to increased levels of toxic metabolic products (such as lactic acid, not measured here), diffusing away from the core cells. This could explain the observed reduction in surface cell viability (25% by day 6) which could not easily be explained by any limitations in O<sub>2</sub> or glucose availability. Indeed, previous research has shown that effective pH buffering reduces cell death by attenuating the acidosis that accompanies anaerobic metabolism (45).

The above findings suggest that when engineering functional tissues, a trade-off needs to be established between the high cell density required and O<sub>2</sub> availability (46). It has thus been suggested that in diffusion-limited tissue constructs, a more sophisticated transport system must be employed (41, 46, 47). Compared to static culture, dynamic perfusion culture has previously been shown to increase gas transport and maintain normoxic levels of O<sub>2</sub> tension within 3D constructs (48, 49). Dynamic perfusion culture (over the outer construct surface) significantly improved core cell viability at day 6, although this remained significantly lower than surface cell viability. It was previously shown that perfusion culture increases cell viability within a construct and improves the spatial uniformity of cell distribution (50-53). Here we have shown that O<sub>2</sub> availability became limiting and impacted on core cell survival in static cultures. Medium perfusion improved core cell viability presumably by increasing O<sub>2</sub> transport, preventing depletion of nutrients at the surface of the construct, as well as by effective removal of harmful metabolic products released by core cells.

## CONCLUSIONS

We have determined parameters for the successful culturing of PSMCs within dense collagen tubular constructs, resulting in prolonged cell survival. The current collagen model establishes that O<sub>2</sub> perfusion is primarily dependent on cellular O<sub>2</sub> consumption and is therefore cell-phenotype and density specific. Our findings suggest that it could be possible to spatially organize cells within 3D constructs to control O<sub>2</sub> distribution throughout the construct, as well as to limit/control O<sub>2</sub> perfusion to certain well-defined construct areas. These controls could potentially act as effectors of metabolic or angiogenic cell signaling.

## ACKNOWLEDGEMENTS

Umber Cheema is a BBSRC David Phillips Fellow and is funded through this route. We are grateful to BBSRC for additional financial support.

We would also like to thank Dr Sue Hall for kindly providing us with PSMCs.

**Conflict of interest statement:** None of the authors have any conflict of interest to report.

Address for correspondence:  
Robert A. Brown  
UCL-TREC, Institute of Orthopaedics, RNOH  
Stanmore Campus  
London, UK HA7 4LP  
e-mail: rehkrab@ucl.ac.uk

## REFERENCES

- Isenberg BC, Williams C, Tranquillo RT. Small-diameter artificial arteries engineered in vitro. *Circ Res* 2006; 98: 25-35.
- L'Heureux N, Dusserre N, Marini A, Garrido S, de la Fuente LM, McAllister T. Technology insight: the evolution of tissue-engineered vascular grafts-from research to clinical practice. *Nat Clin Pract Cardiovasc Med* 2007; 4: 389-95.
- Yang J, Yamato M, Shimizu T, et al. Reconstruction of functional tissues with cell sheet engineering. *Biomaterials* 2007; 28: 5033-43.
- L'Heureux N, Dusserre N, Konig G, Victor B, Keire P, Wight TN, Chronos NA, Kyles AE, Gregory CR, Hoyt G, Robbins RC, McAllister TN. Human tissue-engineered blood vessels for adult arterial revascularization. *Nat Med* 2006; 12: 361-5.
- Laflamme K, Roberge CJ, Pouliot S, Orleans-Juste P, Auger FA, Germain L. Tissue-engineered human vascular media produced in vitro by the self-assembly approach present functional properties similar to those of their native blood vessels. *Tissue Eng* 2006; 12: 2275-81.
- Schmidt CE, Baier JM. Acellular vascular tissues: natural biomaterials for tissue repair and tissue engineering. *Biomaterials* 2000; 21: 2215-31.
- Dahl SL, Koh J, Prabhakar V, Niklason LE. Decellularized native and engineered arterial scaffolds for transplantation. *Cell Transplant* 2003; 12: 659-66.
- Niklason LE, Gao J, Abbott WM, et al. Functional arteries grown in vitro. *Science* 1999; 284: 489-93.
- Jiang HM, Grinnell F. Cell-matrix entanglement and mechanical anchorage of fibroblasts in three-dimensional collagen matrices. *Mol Biol Cell* 2005; 16: 5070-6.
- Grinnell F. Fibroblast biology in three-dimensional collagen matrices. *Trends Cell Biol* 2003; 13: 264-9.
- Lee J, Cuddihy MJ, Kotov NA. Three-dimensional cell culture matrices: state of the art. *Tissue Eng Part B Rev* 2008; 14: 61-86.
- Brown RA, Wiseman M, Chuo CB, Cheema U, Nazhat SN. Ultrarapid engineering of biomimetic materials and tissues: Fabrication of nano- and microstructures by plastic compression. *Adv Funct Mater* 2005; 15: 1762-70.
- Cheema U, Brown RA, Alp B, MacRobert AJ. Spatially defined oxygen gradients and vascular endothelial growth factor expression in an engineered 3D cell model. *Cell Mol Life Sci* 2008; 65: 177-86.
- Gillette BM, Jensen JA, Tang B, Yang GJ, Bazargan-Lari A, Zhong M, Sia SK. In situ collagen assembly for integrating microfabricated three-dimensional cell-seeded matrices. *Nat Mater* 2008; 7: 636-40.
- Jakab K, Neagu A, Mironov V, Markwald RR, Forgacs G. Engineering biological structures of prescribed shape using self-assembling multicellular systems. *Proc Natl Acad Sci U S A* 2004; 101: 2864-9.
- Cheema U, Yang SY, Mudera V, Goldspink GG, Brown RA. 3-D in vitro model of early skeletal muscle development. *Cell Motil Cytoskeleton* 2003; 54: 226-36.
- Volkmer E, Drosse I, Otto S, Stangelmayer A, Stengele M, Kallukalam BC, Mutschler W, Schieker M. Hypoxia in static and dynamic 3D culture systems for tissue engineering of bone. *Tissue Eng Part A* 2008; 14: 1331-40.
- Radisic M, Malda J, Epping E, Geng WL, Langer R, Vunjak-Novakovic G. Oxygen gradients correlate with cell density and cell viability in engineered cardiac tissue. *Biotechnol Bioeng* 2006; 93: 332-43.
- Zhou S, Cui Z, Urban JPG. Nutrient gradients in engineered cartilage: Metabolic kinetics measurement and mass transfer modeling. *Biotechnol Bioeng* 2008; 101: 408-21.
- Mehta G, Mehta K, Sud D, et al. Quantitative measurement and control of oxygen levels in microfluidic poly(dimethylsiloxane) bioreactors during cell culture. *Biomed Microdevices* 2007; 9: 123-34.
- Kellner K, Liebsch G, Klimant I, Wolfbeis OS, Blunk T, Schulz MB, Gopferich A. Determination of oxygen gradients in engineered tissue using a fluorescent sensor. *Biotechnol Bioeng* 2002; 80: 73-83.
- Tsai AG, Johnson PC, Intaglietta M. Oxygen gradients in the microcirculation. *Physiol Rev* 2003; 83: 933-63.
- Okazaki KM, Maltepe E. Oxygen, epigenetics and stem cell fate. *Regen Med* 2006; 1: 71-83.
- Semenza GL. Hypoxia-inducible factor 1: master regulator of O<sub>2</sub> homeostasis. *Curr Opin Genet Dev* 1998; 8: 588-94.
- Hobo K, Shimizu T, Sekine H, Shin'oka T, Okano T, Kurosawa H. Therapeutic angiogenesis using tissue engineered human smooth muscle cell sheets. *Arterioscler Thromb Vasc Biol* 2008; 28: 637-43.
- Hoeben A, Landuyt B, Highley MS, Wildiers H, Van Oosterom AT, De Bruijn EA. Vascular endothelial growth factor and angiogenesis. *Pharmacol Rev* 2004; 56: 549-80.
- Hall SM, Soueid A, Smith T, Brown RA, Haworth SG, Mudera V. Spatial differences of cellular origins and in vivo hypoxia modify contractile properties of pulmonary artery smooth muscle cells: lessons for arterial tissue engineering. *J Tissue Eng Regen Med* 2007; 1: 287-95.
- Li SH, Fan YS, Chow LH, Van Den Diepstraten C, van der Veer E, Sims SM, Pickering JG. Innate diversity of adult human arterial smooth muscle cells - Cloning of distinct subtypes from the internal thoracic artery. *Circ Res* 2001; 89: 517-25.
- Sartore S, Franch R, Roelofs M, Chiavegato A. Molecular and cellular phenotypes and their regulation in smooth muscle. *Rev Physiol Biochem Pharmacol* 1999; 134: 235-320.
- Bailly K, Ridley AJ, Hall SM, Haworth SG. RhoA activation by hypoxia in pulmonary arterial smooth muscle cells is age and site specific. *Circ Res* 2004; 94: 1383-91.
- Nerem RM, Seliktar D. "Vascular Tissue Engineering". *Annu Rev Biomed Eng* 2001; 3: 225-43.
- Griffith CK, Miller C, Sainson RC, et al. Diffusion limits of an in vitro thick prevascularized tissue. *Tissue Eng* 2005; 11: 257-66.
- Bywaters EG. The metabolism of joint tissues. *J Pathol Bact* 1937; 44: 247-68.
- Bibby SR, Jones DA, Ripley RM, Urban JP. Metabolism of the intervertebral disc: Effects of low levels of oxygen,

- glucose, and pH on rates of energy metabolism of bovine nucleus pulposus cells. *Spine* 2005; 30: 487-96.
35. Kumar VB, Viji RI, Kiran MS, Sudhakaran PR. Endothelial cell response to lactate: implication of PAR modification of VEGF. *J Cell Physiol* 2007; 211: 477-85.
  36. Mac Gabhann F, Ji JW, Popel AS. VEGF gradients, receptor activation, and sprout guidance in resting and exercising skeletal muscle. *J Appl Physiol* 2007; 102: 722-34.
  37. Yang J, Yamato M, Kohno C, Nishimoto A, Sekine H, Fukai F, Okano T. Cell sheet engineering: recreating tissues without biodegradable scaffolds. *Biomaterials* 2005; 26: 6415-22.
  38. Dahl SL, Vaughn ME, Hu JJ, Driessen NJ, Baaijens FP, Humphrey JD, Niklason LE. A Microstructurally Motivated Model of the Mechanical Behavior of Tissue Engineered Blood Vessels. *Ann Biomed Eng* 2008; 36: 1782-92.
  39. Hadjipanayi E, Mudera V, Brown RA. Close dependence of fibroblast growth on collagen scaffold matrix stiffness. *J Tissue Eng Regen Med* 2009; 3: 77-84.
  40. Wakatsuki T, Kolodney MS, Zahalak GI, Elson EL. Cell mechanics studied by a reconstituted model tissue. *Biophys J* 2000; 79: 2353-68.
  41. Malda J, Klein TJ, Upton Z. The roles of hypoxia in the in vitro engineering of tissues. *Tissue Eng* 2007; 13: 2153-62.
  42. Smith MK, Mooney DJ. Hypoxia leads to necrotic hepatocyte death. *J Biomed Mater Res A* 2007; 80A: 520-9.
  43. Rong Z, Cheema U, Vadgama P. Needle enzyme electrode based glucose diffusive transport measurement in a collagen gel and validation of a simulation model. *Analyst* 2006; 131: 816-21.
  44. Esumi H, Izuishi K, Kato K, et al. Hypoxia and nitric oxide treatment confer tolerance to glucose starvation in a 5'-AMP-activated protein kinase-dependent manner. *J Biol Chem* 2002; 277: 32791-8.
  45. Brown DA, MacLellan WR, Dunn JCY, Wu BM, Beygui RE. Hypoxic cell death is reduced by pH buffering in a model of engineered heart tissue. *Artif Cells Blood Substit Immobil Biotechnol* 2008; 36: 94-113.
  46. Brown DA, MacLellan WR, Laks H, Dunn JC, Wu BM, Beygui RE. Analysis of oxygen transport in a diffusion-limited model of engineered heart tissue. *Biotechnol Bioeng* 2007; 97: 962-75.
  47. Martin Y, Vermette P. Bioreactors for tissue mass culture: Design, characterization, and recent advances. *Biomaterials* 2005; 26: 7481-503.
  48. Chan KY, Fujioka H, Hirshl RB, Bartlett RH, Grotberg JB. Pulsatile blood flow and gas exchange across a cylindrical fiber array. *J Biomech Eng* 2007; 129: 676-87.
  49. Wendt D, Stroebel S, Jakob M, John GT, Martin I. Uniform tissues engineered by seeding and culturing cells in 3D scaffolds under perfusion at defined oxygen tensions. *Biorheology* 2006; 43: 481-8.
  50. Raimondi MT, Boschetti F, Falcone L, Migliavacca F, Remuzzi A, Dubini G. The effect of media perfusion on three-dimensional cultures of human chondrocytes: integration of experimental and computational approaches. *Biorheology* 2004; 41: 401-10.
  51. Dvir T, Benishti N, Shachar M, Cohen S. A novel perfusion bioreactor providing a homogenous milieu for tissue regeneration. *Tissue Eng* 2006; 12: 2843-52.
  52. Xie Y, Hardouin P, Zhu Z, Tang T, Dai K, Lu J. Three-dimensional flow perfusion culture system for stem cell proliferation inside the critical-size beta-tricalcium phosphate scaffold. *Tissue Eng* 2006; 12: 3535-43.
  53. Carrier RL, Rupnick M, Langer R, Schoen FJ, Freed LE, Vunjak-Novakovic G. Perfusion improves tissue architecture of engineered cardiac muscle. *Tissue Eng* 2002; 8: 175-88.